ARCHIVES OF ELECTRICAL ENGINEERING VOL. 71(2), pp. 409–424 (2022)

DOI 10.24425/aee.2022.140719

Research on the output characteristics of photovoltaic arrays under partial shading conditions based on peak point approximate calculation method

LIMING WEI, KAIKAI LI ✉

School of Electrical and Computer Engineering, Jilin Jianzhu University
Changchun, Jilin, China
e-mails: 982396524@qq.com, ✉kkli2021@163.com

(Received: 12.10.2021, revised: 10.01.2022)

Abstract: The mismatch effect of photovoltaic (PV) arrays due to different illumination intensity has a significant impact on the output characteristics and output power of PV arrays, which is crucial to understand the output characteristics of PV arrays and optimize the array configuration in order to improve the value of the maximum power point. This paper illustrates the short-circuit current mismatch of series circuits, and the open-circuit voltage mismatch of parallel circuits and proposes corresponding solutions for each mismatch phenomenon. The output characteristics of multi-stage series PV arrays and multi-stage parallel PV arrays under complex illumination are analyzed by using the peak point approximation calculation method, and the distribution law of peak voltage points as well as the *I–V* (Current-Voltage) characteristic equation of each operating section are proposed. On this basis, the output characteristics of 3×3 centralized PV arrays are analyzed and verified by simulation. By comparing series and parallel PV arrays with the same condition, as well as several groups of centralized PV arrays with the same topology and different types of illumination distribution, this paper proposes a configuration optimization method for PV arrays. Matlab/Simulink simulation results confirm that the output power of parallel arrays is greater than that of series arrays under the same configuration and illuminationt distribution type, and the peak point is less than that of series arrays under the same configuration and lighting conditions; while in centralized PV arrays, the fewer series modules are shaded, the greater the output power and the less the peak point.

Key words: *I–V* characteristic equation, peak point approximate calculation method, peak voltage point, shadow occlusion's rate, type of illumination distribution

1. Introduction

Solar power generation has been widely used since its advantages such as rich resources, pollution-free gas emission, and so on. Since solar energy is a promising option of renewable energy [1]. However, due to the change of solar altitude angle and solar azimuth angle at any time in a day, the solar panel can not always be in the external environment of uniform illumination, so there will always exist a local shadow effect [2]. A photovoltaic (PV) array with local shadow will lead to a serious mismatch effect, it causes large power loss and increases the cost of photovoltaic power generation [3].

In order to reduce the local shadow effect effectively, there are two main methods [4]. First, calculate local declination angle, solar time angle, solar zenith angle, and other data, then design the number, spacing, azimuth angle, tilt angle, and other parameters of the photovoltaic panel reasonably, so as to obtain the maximum solar radiation and minimize the local shadow effect. Second, obtain the output characteristic's curve of the photovoltaic array under complex illumination through the computer simulation software, and find the most suitable topology structure's type and installation's mode of the photovoltaic array, in order to achieve the best output effect of the photovoltaic panel. A dynamic reconstruction technique is proposed to increase the maximum power in partial shading conditions [5]. In [6], the L-shaped propagated array configuration method with a new dynamic reconfiguration algorithm has been proposed for enhancing the energy conversion under partial shading conditions, it alleviates the mismatch loss by evenly distributing partial shadows over the PV array. In [7], a method is proposed to reduce the power loss of solar photovoltaic systems which is under partial shadow conditions by using Re-Allocation of PV module-fixed electrical connections. In [8], the author studied four different system configurations, the derivation for the explicit expression of mean time to system failure, steady-state availability and cost-benefit analysis were performed. In [9], the author studied causes of the hot spot phenomenon and analyzed the output characteristics of photovoltaic arrays under shadow conditions. In [10], the author pointed out that partial shading conditions instigate the mismatch in the PV electrical characteristics and it induces the degradation in PV output energy. The amount of the mismatch depends upon various aspects such as array size, configuration type, and shading patterns. In [11], the author built the model of the photovoltaic array under the shadow condition and carried out several simulations, and got some characteristics of the P–V (Power-Voltage) curve and the I–V (Current-Voltage) curve. The above research provided a theoretical basis for the maximum power point tracking (MPPT) under the shadow condition. After understanding the output characteristics of photovoltaic arrays, we can start to design the maximum power point tracking control strategy. For example, a novel golden section search assisted perturb and observe (GSS-PO) hybrid algorithm is proposed to solve the problems of the conventional PO (CPO), the new algorithm has a very low convergence time and a very high tracking efficiency and accuracy [12]. However, the above characteristic analysis of the photovoltaic array is not perfect, and the corresponding photovoltaic array configuration optimization method is not proposed based on the output characteristics.

Combined with previous studies, in order to understand the output characteristics of the photovoltaic array and optimize the configuration of the photovoltaic array, to make the output power of the photovoltaic array as large as possible, this paper studies the output characteristics of the photovoltaic array with local shadow, while the configuration of the photovoltaic array

is optimized to obtain higher output power. The simulation results based on Matlab/Simulink show that the theoretical research is correct and the proposed photovoltaic array configuration optimization measures are effective.

This paper is divided into five sections. Section 2 is about the mismatch effect, which introduces the influence of two different types of mismatch effects on the output of the photovoltaic array. Section 3 is the analysis of the output characteristics of the photovoltaic array, which analyzes the output characteristics of series arrays and parallel arrays, and gives the characteristic equations of each working stage. Section 4 is about the output characteristics and configuration optimization of the centralized photovoltaic array. The method of configuration optimization is proposed and verified by simulation. Section 5 is the summary of the full paper.

2. Mismatch effect of photovoltaic array

2.1. Short-circuit current mismatch in series circuit

Mismatch loss is caused by different parameters of interconnected batteries or components, such as different short-circuit currents or open-circuit voltage. Generally, the short-circuit current mismatch of series circuits is common, which is easily caused by the phenomenon of local shadow. For such type of mismatch, the bypass diode is usually connected at both ends of the occluded battery, so that the current from a normal battery can flow through the branch of the bypass diode. The specific connection diagram of the bypass diode is shown in Fig. 1.

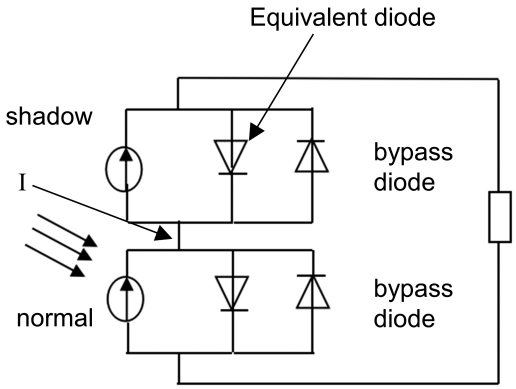

Fig. 1. Bypass diode in series circuit

As shown in the figure above, if one battery is under normal illumination, its generated photocurrent is I_{PH_N}, and the other battery is occluded, its generated photocurrent is I_{PH_S}, $I_{PH\_N} > I_{PH\_S}$. Because the current of the constant current source is unchangeable, the current $I = I_{PH\_N} - I_{PH\_S}$ will flow to the bypass diode, which locates at both ends of the occluded battery. If no bypass diode is installed, it can only flow to the equivalent diode of the occluded battery's side, so that the occluded battery is in the state of reverse bias voltage. If the voltage is greater than the reverse breakdown voltage, the battery will be burned. Therefore, the bypass diode can effectively prevent the occurrence of a short-circuit current mismatch in the series circuit.

2.2. Open-circuit voltage mismatch in parallel circuit

If the battery of any of the two photovoltaic modules in parallel is occluded, the open-circuit voltage mismatch of the parallel circuit will occur. For such type of mismatch, the blocking diode is usually installed to avoid the damage caused by the mismatch. The specific blocking diode's connection diagram is shown in Fig. 2.

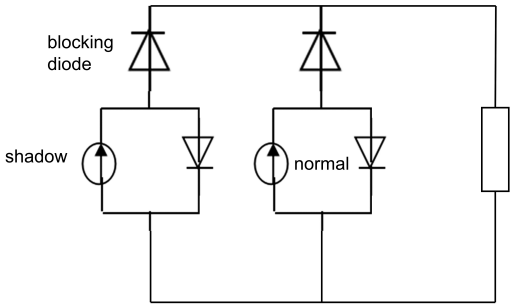

Fig. 2. Blocking diode in parallel circuit

As shown in the figure above, if one battery is under normal illumination, its generated photocurrent is $V_{\mathrm{PH\_}N}$, and the other battery is occluded, its generated photocurrent is $V_{\mathrm{PH\_}S}$, $V_{\mathrm{PH\_}N} > V_{\mathrm{PH\_}S}$, the blocked PV module will be subjected to a reverse voltage, $V = V_{\mathrm{PH\_}N} - V_{\mathrm{PH\_}S}$. This causes current to flow into the left battery, the current will pass through the bypass diode connected with it. If the rated current of the bypass diode is small, the diode will not be able to bear the quantity of electric charge and will generate heat, then the diode is more possible to be burned. Therefore, the blocking diode and bypass diode with a high rated current are usually installed to prevent the open-circuit voltage mismatch of the parallel circuit caused by local shadow.

3. Analysis of the output characteristics of photovoltaic arrays

3.1. Output characteristics of multistage series photovoltaic array

In the environment of uniform illumination, each cell in the series photovoltaic array accepts the same illumination's intensity, each cell produces the same photocurrent and outputs the same voltage, the bypass diode in parallel with the cell is in the blocking state. However, if any cells are occluded, the output characteristics of the series photovoltaic array will no longer remain in the original state.

It is assumed that the series photovoltaic array consists of N batteries, each battery is in parallel with a bypass diode. M batteries are under illumination, and $(N - M)$ batteries are occluded, the illumination's intensity of the battery under normal illumination is G_N, and the illumination's intensity of the occluded battery is G_S, $G_N > G_S$. The photocurrent generated by the battery under normal illumination is $I_{\mathrm{PH\_}N}$, its short-circuit current is $I_{\mathrm{SC\_}N}$, the photocurrent generated by the occluded battery is $I_{\mathrm{PH\_}S}$, its short-circuit current is $I_{\mathrm{SC\_}S}$, $I_{\mathrm{PH\_}N} > I_{\mathrm{PH\_}S}$, $I_{\mathrm{SC\_}N} > I_{\mathrm{SC\_}S}$.

Under complex illumination, the working state of the series photovoltaic array can be divided into two stages, each stage shows different working characteristics [13, 14].

In the first stage, when the output current $I \in (I_{SC\_S},\ I_{SC\_N}]$, all the batteries under normal illumination work, the output voltage of a single battery under normal illumination is expressed as follows:

$$V_{\text{module\_}N} = \frac{1}{M}\left[V + (N-M)V_{\text{by}}\right]. \tag{1}$$

In the above formula, V_{by} represents the generated voltage of the bypass diode at both ends of the occluded battery when the bypass diode is turned on. The expression of V_{by} is as follows [13]:

$$V_{\text{by}} = \frac{n_{\text{by}} \cdot k \cdot T_{\text{by}}}{q} \text{In}\left(\frac{I - I_{\text{PH\_}S}}{I_{\text{oby}}} + 1\right). \tag{2}$$

In the above formula, $n_{\text{by}}, T_{\text{by}}$, and I_{oby}, respectively, represent the ideal factor, temperature, and reverse saturation current of the bypass diode. k represents the Boltzmann constant, q represents the unit electric charge. In the first stage, the output current's equation of the series photovoltaic array is as follows [13]:

$$I = I_{\text{PH\_}N} - I_{\text{O}}\left\langle \exp\left\{\frac{q}{nkT}\left[\frac{V}{M} + \frac{(N-M)V_{\text{by}}}{M} + IR_s\right]\right\} - 1\right\rangle. \tag{3}$$

In the above formula, I_{O}, n, respectively, represents the reverse saturation current and characteristic factor of the equivalent diode, T represents the temperature of the battery. Combining Formula (1) – Formula (3), it can be noticed that the output voltage's equation of the series photovoltaic array in the first stage is expressed as follows:

$$V = M \cdot \left[\frac{nkT}{q} \ln\left(\frac{I_{\text{PH\_}N} - I}{I_{\text{O}}} + 1\right) - IR_S\right] - (N-M) \cdot \frac{n_{\text{by}} \cdot k \cdot T_{\text{by}}}{q} \ln\left(\frac{I - I_{\text{PH\_}S}}{I_{\text{oby}}} + 1\right). \tag{4}$$

According to the principle of the constant voltage method, there is a certain proportion coefficient between photovoltaic cell's peak voltage and photovoltaic cell's open-circuit voltage, which is generally from 0.7 to 0.8. If there is a constant c_N, the relationship between the peak voltage and open-circuit voltage of the battery under illumination can be expressed as follows:

$$V_{\text{MPP\_}N} = c_N \cdot V_{\text{OC\_}N}. \tag{5}$$

In the current range $(I_{SC\_S},\ I_{SC\_N}]$, when the cells under illumination output power reach their maximum power point, the series photovoltaic array will reach the first maximum power point. The voltage and power of this point can be expressed by the following relationship:

$$V_{\text{array\_MPP1}} = M \cdot c_N \cdot V_{\text{OC\_}N} - (N-M)V_{\text{by}}, \tag{6}$$

$$P_{\text{array\_MPP1}} = \sum_{i=1}^{M} P_{\text{MPP\_}i}. \tag{7}$$

In Formula (7), $P_{\text{MPP}N\_i}$ represents the maximum power of a single-cell under illumination. In the second stage, when the output current $I \in [0,\ I_{SC\_S}]$, all the cells work together, and each bypass diode that is connected at both ends of the occluded cell is in the

non-conduction state. At this time, the voltage's expression of the series photovoltaic array is:

$$\begin{aligned} V &= MV_{\text{module\_}N} + (N-M)V_{\text{module\_}S} \\ &= \frac{nkTM}{q}\text{In}\left(\frac{I_{\text{PH\_}N}-I}{I_{\text{O}}}+1\right) + \frac{nkT}{q}(N-M)\text{In}\left(\frac{I_{\text{PH\_}N}-I}{I_{\text{O}}}+1\right) - NIR_{\text{S}}\,. \end{aligned} \tag{8}$$

It is assumed that $I_{\text{MPP\_}S}$ is the maximum power point's current of the occluded battery. In the current range $[I_{\text{MPP\_}S}, I_{\text{SC\_}S}]$, the output voltage of all the batteries under illumination increases slowly, and the output power of all the batteries under illumination decreases slowly, while the output power of all the occluded batteries increases rapidly. When I is equal to $I_{\text{MPP\_}S}$, all the occluded batteries reach their maximum power point. At this time, the series photovoltaic array reaches the second maximum power point, the voltage and power of this point can be expressed by the following relationships:

$$V_{\text{array\_MPP2}} = M \cdot x_1 V_{\text{OC\_}N} + (N-M)c_s \cdot V_{\text{OC\_}S}\,, \tag{9}$$

$$P_{\text{array\_MPP2}} = \sum_{i=1}^{M} P_i + \sum_{j=1}^{N-M} P_{\text{MPP}S\_j}\,. \tag{10}$$

In Formula (9), $V_{\text{OC\_}S}$ represents the open-circuit voltage of the occluded battery and c_s represents the ratio coefficient between the occluded battery's maximum power point voltage and occluded battery's open-circuit voltage. x_1 is the constant, $c_N < x_1 < 1$. In Formula (10), $P_{\text{MPP}S\_j}$ represents the maximum power of a single occluded battery, and $\sum_{i=1}^{M} P_i$ represents the sum of power of all the batteries under illumination when the system reaches the second maximum power point. In the current range $[0, I_{\text{MPP\_}S}]$, the output power of all batteries drops rapidly, which makes the output power of the system also drop rapidly until all batteries no longer work. To sum up, when $(N-M)$ cells are occluded, the series photovoltaic array composed of N cells has two peak voltage points and two working ranges, each range shows a different I–V characteristic expression.

3.2. Output characteristics of mult-istage parallel photovoltaic array

In the environment of uniform illumination, each cell in the parallel photovoltaic array accepts the same illumination's intensity, each cell outputs the same voltage, and the blocking diode in series with the cell is conductive. However, if any cell is occluded, the output characteristics of the parallel photovoltaic array will no longer remain in the original state.

It is assumed that the parallel photovoltaic array consists of N batteries, each battery is in series with a blocking diode, M batteries are under illumination, and $(N-M)$ batteries are occluded, the illumination's intensity of the battery under normal illumination is G_N, and the illumination's intensity of the occluded battery is G_S, $G_N > G_S$. The photocurrent generated by the battery under normal illumination is $I_{\text{PH\_}N}$, its open-circuit voltage is $V_{\text{OC\_}N}$, the photocurrent generated by the occluded battery is $I_{\text{PH\_}S}$, its open-circuit voltage is $V_{\text{OC\_}S}$, $I_{\text{PH\_}N} > I_{\text{PH\_}S}$, $V_{\text{OC\_}N} > V_{\text{OC\_}S}$.

Under complex illumination, the working state of the parallel photovoltaic array can be divided into two stages, each stage shows different working characteristics [15].

In the first stage, when the output voltage $V \in [0, V_{OC\_S}]$, all the cells output power together. The output current's equation of the parallel photovoltaic array can be expressed by the following relationship:

$$I = MI_{module\_N} + (N - M)I_{module\_S}\,. \tag{11}$$

The output current of the battery under the illumination I_{module_N} and the output current of the occluded battery I_{module_S} is expressed as follows [15]:

$$I_{module\_N} = I_{PH\_N} - I_O\left\{\exp\left[\frac{q}{nkT}\left(V_{module\_N} + I_{module\_N}R_S\right)\right] - 1\right\}, \tag{12}$$

$$I_{module\_S} = I_{PH\_S} - I_O\left\{\exp\left[\frac{q}{nkT}\left(V_{module\_S} + I_{module\_S}R_S\right)\right] - 1\right\}. \tag{13}$$

In the above formula, V_{module_N} and V_{module_S}, respectively, represent the output voltage of the battery under illumination and the output voltage of the occluded battery. In addition, the relationship among the parallel photovoltaic array's output voltage V and V_{module_N} as well as V_{module_N} can be expressed as follows:

$$V = V_{module\_N} - V_{block\_N} = V_{module\_S} - V_{block\_S}\,. \tag{14}$$

In the above formula, V_{block_S} represents the voltage of the blocking diode connected with the occluded battery and V_{block_N} represents the voltage of the blocking diode connected with the battery under illumination. V_{block_S} and V_{block_N} can be expressed by the following relationship [13]:

$$V_{block\_N} = \frac{nkT \cdot n_{block}}{q}\left(\frac{I_{module\_N}}{I_{oblock}} + 1\right), \tag{15}$$

$$V_{block\_S} = \frac{nkT \cdot n_{block}}{q}\left(\frac{I_{module\_S}}{I_{oblock}} + 1\right). \tag{16}$$

In the above formula, I_{oblock} and n_{block}, respectively, represent the blocking diode's reverse saturation current and blocking diode's ideal factor. Combining Formulas (11)–(16), the output current's equation of the parallel photovoltaic array in the first stage is as follows:

$$I = (N - M)\cdot\left\langle I_{PH\_S} - I_O\left\{\exp\left[\begin{array}{c}\frac{q}{nkT}\left(V + I_{module\_S}R_S\right)\\ +\frac{n\text{block}}{n}\left(\frac{I_{module\_S}}{I_{oblock}} + 1\right) - 1\end{array}\right]\right\}\right\rangle$$

$$+ M\cdot\left\langle I_{PH\_N} - I\left\{\exp\left[\begin{array}{c}\frac{q}{nkT}\left(V + I_{module\_N}R_S\right)\\ +\frac{n\text{block}}{n}\left(\frac{I_{module\_N}}{I_{oblock}} + 1\right) - 1\end{array}\right]\right\}\right\rangle. \tag{17}$$

Because the change of illumination's intensity has little effect on the voltage parameters of the battery, the maximum power point voltage of the occluded battery V_{MPP_S} is approximately equal to the maximum power point voltage of the battery under illumination V_{MPP_N}, $V_{MPP\_N} < V_{OC\_S}$. V_{OC_S} represents the open-circuit voltage of the occluded battery. The occluded cell reaches the maximum power point earlier compared with the cell under illumination. In the range $[V_{MPP\_S},$

V_{MPP_N}], the output power of the occluded cell decreases nonlinearly and the output power of the cell under illumination rises nonlinearly. At this time, the parallel photovoltaic array reaches its maximum power point. The power of this point can be approximately expressed as:

$$P = \sum_{i=1}^{M} P_{MPP\_i} + \sum_{j=1}^{N-M} P_{MPPS\_j} \,. \tag{18}$$

In the second stage, when the output voltage $V \in (V_{OC\_S}, V_{OC\_N}]$, all the occluded batteries no longer output power, only all the batteries under illumination are in the working state, and the output power of the system gradually decreases until all the batteries no longer work. At this time, the output current's equation of the parallel photovoltaic array can be expressed as follows:

$$I = M \cdot \left\langle I_{PH\_N} - I_O \left\{ \exp\left[\frac{q}{nkT} \left(V + \frac{IR_S}{M} \right) + \frac{n_{block}}{n} \left(\frac{I}{MI_{oblock}} + 1 \right) \right] - 1 \right\} \right\rangle . \tag{19}$$

To sum up, when $(N - M)$ cells are occluded, the parallel photovoltaic array composed of N cells has one peak voltage point and two working ranges, each range shows a different I–V characteristic expression.

4. Output characteristic analysis and configuration optimization of centralized photovoltaic array

4.1. Output characteristics of multi-stage centralized photovoltaic array

4.1.1. 3 × 3 centralized photovoltaic array

As shown in Fig. 3, a centralized photovoltaic array with three types of illumination distribution is demonstrated as an example in this paper. This photovoltaic array's output characteristics

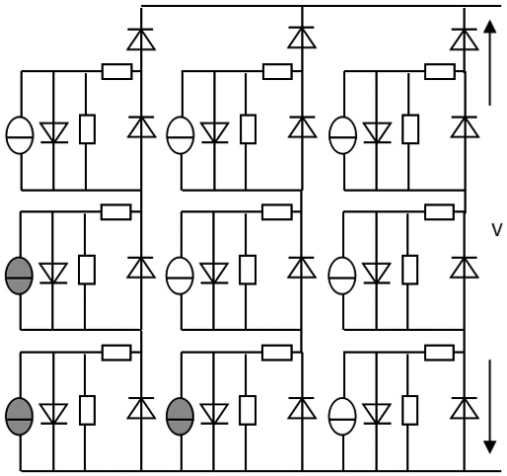

Fig. 3. Structure model of 3 × 3 centralized photovoltaic array

is analyzed as well. It is assumed that the illumination intensity of the battery under normal illumination is G_N. In addition, the illumination intensity of the occluded battery is G_S. The model of this specific photovoltaic array is shown in Fig. 3 and the key parameters in this model are defined and discussed in this section.

In order to guide the audience and define units, it is assumed that V_{OC_N} represents the open-circuit voltage of the battery under illumination, c_N represents the ratio coefficient between the maximum power point voltage of the battery under illumination and the open-circuit voltage of the battery under illumination, I_{SC_N} represents the short-circuit current of the battery under illumination. Meanwhile, V_{OC_S} represents the open-circuit voltage of the occluded battery, c_S represents the ratio coefficient between the maximum power point voltage of the occluded battery and the open-circuit voltage of the occluded battery, I_{SC_S} represents the short-circuit current of the occluded battery.

In addition, the voltage of each bypass diode is defined as V_{by} and the voltage of the blocking diode connected with the i-th group of a series photovoltaic array is defined as V_{block_i}. In this paper, the output voltage of 3×3 photovoltaic arrays is divided into three independent intervals, which are $[0, 2V_{OC\_S} + V_{OC\_N}]$, $[2V_{OC\_S} + V_{OC\_N}, 2V_{OC\_N} + V_{OC\_S}]$, $[2V_{OC\_N} + V_{OC\_S}, 3V_{OC\_N}]$. In each voltage range, the output current of each series photovoltaic array can also be divided into two intervals which are $[I_{SC\_S}, I_{SC\_N}]$ and $[0,\ I_{SC\_S}]$.

The 3×3 photovoltaic array has its maximum power point only in the voltage range of $[0, 2V_{OC\_S} + V_{OC\_N}]$, based on the fundamental theories. Therefore, this paper analyses the output characteristics in this range. In the beginning stage, the first series photovoltaic array reaches its maximum power point and its maximum power point's voltage can be expressed as:

$$V_{array1\_mpp\_1} = c_N V_{OC\_N} - 2V_{by} - V_{block\_1}\,. \tag{20}$$

On the right side of this point, the output power of the second and third series photovoltaic array is still increasing, while the output power of the first series photovoltaic array is gradually decreasing until its output current enters the range from $[I_{SC\_S},\ I_{SC\_N}]$ into $[0, I_{SC\_S}]$. At this time, the photovoltaic array reaches the first maximum power point as $V_{system\_MPP\_1}$. It is approximately equal to $V_{array1\_MPP\_1}$, and the corresponding output power can be expressed as:

$$P_1 = P_{array1\_MPPN} + 2P_{array2\_N} + 3P_{array3\_N}\,. \tag{21}$$

As the system's output voltage increases, the second series photovoltaic array reaches its maximum power point voltage which is expressed as:

$$V_{array2\_MPP\_1} = 2c_N V_{OC\_N} - V_{by} - V_{block\_2}\,. \tag{22}$$

Then, on the right side of this point, the output power of the first and third series photovoltaic array is still increasing, while the output power of the second series photovoltaic array is gradually decreasing until its output current enters the range from $[I_{SC\_S}, I_{SC\_N}]$ into $[0, I_{SC\_S}]$. At this time, the photovoltaic array reaches the second maximum power point $V_{system\_MPP\_2}$. It is approximately equal to $V_{array2\_MPP\_1}$. The corresponding power can be expresed as:

$$P_2 = P_{array1\_N} + 2P_{array1\_S} + 2P_{array2\_MPPN} + 3P_{array3\_N}\,. \tag{23}$$

Afterward, the first series photovoltaic array and the second series photovoltaic array, respectively, reaches their second maximum power points. The maximum power point's voltages are shown as:

$$\begin{aligned} V_{\text{array1\_MPP\_2}} &= x_1 V_{\text{OC\_}N} + 2c_s V_{\text{OC\_}S} - V_{\text{block\_1}}\,, \quad c_N < x_1 < 1, \\ V_{\text{array2\_MPP\_2}} &= 2x_2 V_{\text{OC\_}N} + c_s V_{\text{OC\_}S} - V_{\text{block\_2}}\,, \quad c_S < x_2 < 1. \end{aligned} \tag{24}$$

The third series photovoltaic array also reaches its first maximum power point which is:

$$V_{\text{array3\_MPP\_1}} = 3c_N V_{\text{OV\_}N} - V_{\text{block\_3}}\,. \tag{25}$$

The length of the interval formed by the above three peak voltage points is very short, and the 3×3 photovoltaic array shows system's maximum power point in this interval. The corresponding output power can be expressed below and the result of $P_1 < P_3 < P_2$ can be obtained in this way. In the next section, the simulation results will be discussed based on experiments.

$$P_3 = P_{\text{array1\_}N} + 2P_{\text{array1\_MPP}S} + 2P_{\text{array2\_}N} + P_{\text{array2\_MPP}S} + 3P_{\text{array3\_MPP}N}\,. \tag{26}$$

4.1.2. Simulation result

The output characteristics of the photovoltaic array mentioned above are simulated as key paramters by using the solar toolbox of PVsyst. The photovoltaic cell module adopted in this paper, which is 3E−STK−120P6A, is the basic component of the photovoltaic array. Its open-circuit voltage is 20.7 V and its maximum power point voltage is 16.8 V. Besides, the shading rate is set as 80% and the intensity of normal illumination is 1000 W/m^2. The envrionmental temperature is set as 25°C in this simulation. Then, the result is shown in Fig. 4 after all parameters are set properly.

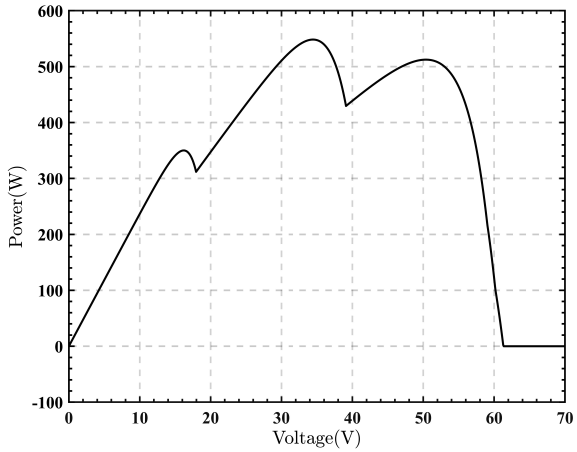

Fig. 4. *P–V* curve of 3×3 centralized photovoltaic array

According to the previous theoretical analysis, it can be noticed that this centralized photovoltaic array shows three maximum power points. The first peak voltage and seconde peak

voltage are approximately equal to $V_{\text{array1\_MPP\_1}}$ and $V_{\text{array2\_MPP\_1}}$, respectively and the third peak voltage is located in the interval composed of $V_{\text{array1\_MPP\_2}}$, $V_{\text{array2\_MPP\_2}}$, and $V_{\text{array3\_MPP\_3}}$. The relationship among respective corresponding output power can be expressed as $P_1 < P_2 < P_3$. Due to the fact that the value of V_{by} and $V_{\text{block\_}i}$ are too small, they are ignored in the following peak-point approximation calculation method. The specific calculation process is as follows:

$$\begin{aligned}
V_{\text{array1_MPP_1}} &= c_N V_{\text{OC_}N} - 2V_{\text{by}} - V_{\text{block1}} \approx 16.8 \text{ V},\\
V_{\text{array2_MPP_1}} &= 2c_N V_{\text{OC_}N} - V_{\text{by}} - V_{\text{block2}} \approx 33.6 \text{ V},\\
V_{\text{array1_MPP_2}} &= x_1 V_{\text{OC_}N} - 2c_S V_{\text{OC}_S} - V_{\text{block1}} \approx 50.6 \text{ V},\\
V_{\text{array2_MPP_2}} &= 2x_2 V_{\text{OC_}N} - c_S V_{\text{OC}_S} - V_{\text{block2}} \approx 53.3 \text{ V},\\
V_{\text{array3_MPP_1}} &= 3c_N V_{\text{OC_}N} - V_{\text{block3}} \approx 50.4 \text{ V}.
\end{aligned} \tag{27}$$

From the P–V curve obtained in this simulation, it can be noticed that the position of the peak point and the relationship among each peak point's power is basically consistent with the previous theoretical derivation.

4.2. Optimal configuration of photovoltaic array

4.2.1. The output characteristic's comparison between series photovoltaic array and parallel photovoltaic array

According to the previous theoretical analysis, the peak voltage point of the parallel photovoltaic array is located in the range of $[V_{\text{MPP\_}S}, V_{\text{MPP\_}N}]$ when it is under complex illumination. The corresponding maximum power is approximately equal to $\sum_{i=1}^{n} P_{\text{MPP\_}i} + \sum_{j=1}^{m} P_{\text{MPPS\_}j}$ where n represents the number of batteries under illumination, m represents the number of occluded batteries, $P_{\text{MPPN\_}i}$ represents the maximum power of a single battery under illumination and $P_{\text{MPPS\_}j}$ represents the maximum power of a single occluded battery.

If a group of series photovoltaic array has the same topology structure and same type of illumination distribution as the parallel photovoltaic array mentioned above, it will have two maximum power points in total. The first peak voltage, the corresponding power, the second peak voltage and the corresponding power can be expressed as below from Eqs. (28) to (31). It can be seen that the value of $\sum_{i=1}^{n} P_i$ is smaller than the value of $P = \sum_{i=1}^{n} P_{\text{MPP\_}i}$.

$$V_1 = nV_{\text{MPP\_}N} - mV_{\text{by}}\,, \tag{28}$$

$$P_1 = \sum_{i=1}^{n} P_{\text{MPP\_}i}\,, \tag{29}$$

$$V_2 = nx_1 V_{\text{OC\_}N} + mc_S V_{\text{OC\_}S}\,, \tag{30}$$

$$P_2 = \sum_{i=1}^{n} P_i + \sum_{j+1}^{m} P_{\text{MPPS\_}j}\,. \tag{31}$$

Therefore, it can be seen that the parallel photovoltaic array has higher power generation efficiency than the series photovoltaic array with the same topology structure and type of illumination

distribution. It can be verified through the simulation by using Matlab/Simulink. On the main interface of PV cell's electrical property setting, the parallel photovoltaic array and the series photovoltaic array are both set to have 10 cells. There are 6 cells under illumination and the other 4 cells are occluded. Other external parameters are set as unchanged. Then the simulation results of *P–V* curves can be obtained as shown in Fig. 5. The simulation results show that with the same topology structure and same type of illumination distribution, the parallel photovoltaic array not only has higher output power than the series photovoltaic array but also has fewer maximum power points. Thus, its maximum power point can be tracked and be controlled efficiently.

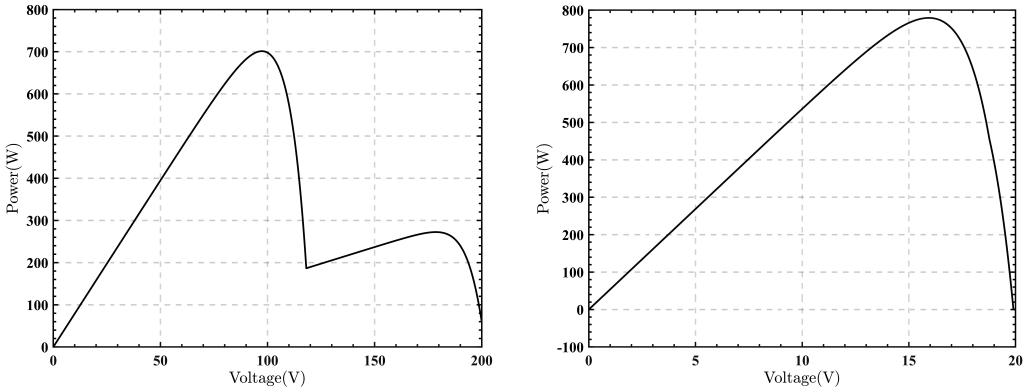

(a) *P–V* curve of series photovoltaic array (b) *P–V* curve of parallel photovoltaic array

Fig. 5. *P–V* curve comparison between series photovoltaic array and parallel photovoltaic array

4.2.2. The output characteristic's comparison of centralized photovoltaic array under different types of illumination's distribution

A centralized photovoltaic array with three different types of illumination's distribution has been researched in this section. The distribution of the three types of illumination is shown in Table 1.

Table 1. Illumination's distribution type of centralized photovoltaic array

Type	***M*1**	N_N	N_S	***M*2**	N_N	N_S	***M*3**	N_N	N_S
I	1	0	4	3	4	0	0	0	0
II	4	3	1	0	0	0	0	0	0
III	2	2	2	1	3	1	1	4	0

As shown above, type I and type II are regular illumination's distribution. Type III is irregular illumination's distribution. Return to the main interface, the model of cell and external parameters are set as unchanged. Then by simulating the *P–V* curve of a 4×4 centralized photovoltaic array under four different types of illumination distribution successively, we obtained curves that are shown in Fig. 6–8.

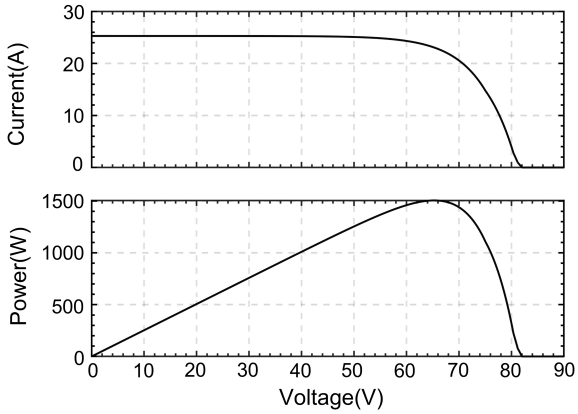

Fig. 6. *P–V* characteristic curve of type I

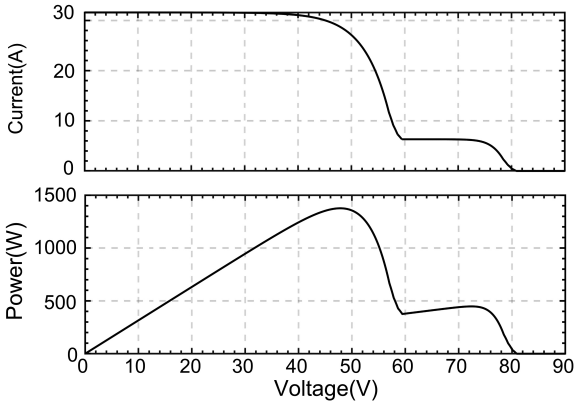

Fig. 7. *P–V* characteristic curve of type II

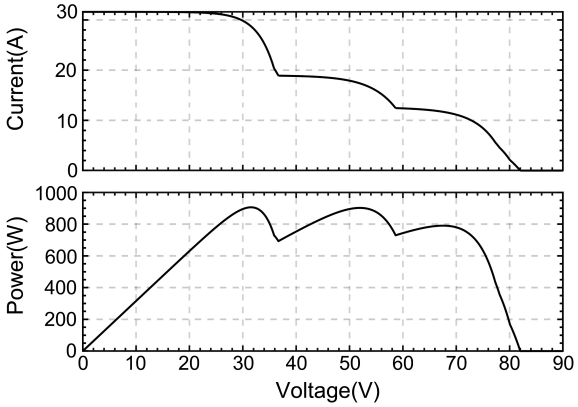

Fig. 8. *P–V* characteristic curve of type III

Based on the curves shown in Figs. 6–8, the centralized photovoltaic array of type I and type II has higher output power and lower peak voltage points than the centralized photovoltaic array of type III. It can be concluded that the centralized photovoltaic array with regular illumination distribution is more suitable for the actual configuration than the centralized photovoltaic array with irregular illumination distribution. Moreover, by comparing type I with type II, type III, it can be concluded that if there are fewer groups of series photovoltaic arrays that contain the occluded cell, the centralized photovoltaic array has fewer maximum power points and has higher output power. By contrast, the maximum current is essentially constant. This is due to the reason that the current output from each branch in a parallel structure remain the same. Also, it varies with voltage. In addition, the *P–V* curve has several peaks while the *I–V* curve has several steps.

To sum up, this paper proposes several measures to optimize the configuration of photovoltaic arrays. Firstly, a parallel photovoltaic array should be organized as the type of topology structure, as it is possible in small PV power generation systems. Secondly, in order to meet the requirements of commercial benefits, bypass diodes and blocking diodes should be installed in the medium-sized photovoltaic power generation systems. The specific number should be consistent with the actual demand. The bypass diodes should be selected with higher rated current. Thirdly, for the large centralized photovoltaic array which are under complex illumination, the shadow should be regularly distributed in a single group of series photovoltaic arrays in order to achieve high efficiency.

5. Conclusions

This paper takes the photovoltaic array under complex illumination as a research object and analyzes two types of mismatch which are a short-circuit current mismatch in a series circuit and an open-circuit voltage mismatch in a parallel circuit. The paper finds out the peak voltage point's distribution rule of multi-stage series photovoltaic arrays as well as the peak voltage point's distribution rule of multi-stage parallel photovoltaic arrays and establishes *I–V* characteristic equations of each working section. Moreover, the paper simulates the *P–V* curve of series photovoltaic arrays and simulates the *P–V* curve of parallel photovoltaic arrays with the same topology structure and the same type of illumination's distribution through PVsyst software, the result indicates that under the same condition, parallel photovoltaic array's output power is higher and the number of parallel photovoltaic array's maximum power points is less. Besides, the paper uses Matlab/Simulink to simulate the *P–V* curve of a 3×3 centralized photovoltaic array with three different types of illumination distribution, so as to verify the correctness of a peak point's approximate calculation method under complex illumination. In addition, the paper obtains the *P–V* curve of a 4×4 centralized photovoltaic array under four different types of illumination's distribution through simulation, the result indicates that when the shadow is regularly distributed and the number of a series photovoltaic array's group that contains occluded cells is less, the output power of the centralized photovoltaic array is higher and the number of centralized photovoltaic array's maximum power points is less.

References

[1] Anurag Singh Yadav, Mukherjee V., *Conventional and advanced PV array configurations to extract maximum power under partial shading conditions: A review*, Renewable Energy, vol. 178, pp. 977–1005 (2021), DOI: 10.1016/j.renene.2021.06.029.

[2] Alivarani Mohapatra, Byamakesh Nayak, Kanungo Barada Mohanty, *Analytical approach to locate multiple power peaks of photovoltaic array under partial shading condition and hybrid array configuration schemes to reduce mismatch losses*, Energy Sources Part a-Recovery Utilization and Environmental Effects (2021), DOI: 10.1080/15567036.2021.1945710.

[3] Kumar Ritesh, Sahu Balakrushna, Shiva Chandan Kumar, Rajender B., *A control topology for frequency regulation capability in a grid integrated PV system*, Archives of Electrical Engineering, vol. 6, no. 2, pp. 389–401 (2020), DOI: 10.24425/aee.2020.133033.

[4] Han Guodong, Hu Lanping, Yang Fucheng *et al.*, *Radiation calculation analysis of photovoltaic power generation system with different installation way*, Yunnan Electric Power, vol. 45, no. 3, pp. 8–10 (2017).

[5] Sai Krishna G., Tukaram Moger, *A novel adaptive dynamic photovoltaic reconfiguration system to mitigate mismatch effects*, Renewable and Sustainable Energy Reviews, vol. 141 (2021), DOI: 10.1016/j.rser.2021.110754.

[6] Srinivasan A., Devakirubakaran S., Meenakshi Sundaram B., Praveen Kumar Balachandran, Santhan Kumar Cherukuri, Prince Winston D., Thanikanti Sudhakar Babu, Hassan Haes Alhelou, *L-Shape Propagated Array Configuration With Dynamic Reconfiguration Algorithm for Enhancing Energy Conversion Rate of Partial Shaded Photovoltaic Systems*, IEEE Access, vol. 9, pp. 97661–97674 (2021), DOI: 10.1109/ACCESS.2021.3094736.

[7] Rupendar Kumar Pachauri, Isha Kansal, Thanikanti Sudhakar Babu, Hassan Haes Alhelou, *Power Losses Reduction of Solar PV Systems Under Partial Shading Conditions Using Re-Allocation of PV Module-Fixed Electrical Connections*, IEEE Access, vol. 9, pp. 94789–94812 (2021), DOI: 10.1109/ACCESS.2021.3093954.

[8] Suleiman K., Ali U.A., Ibrahim Yusuf, Koko A.D., Bala S.I., *Comparison between four dissimilar solar panel configurations*, Journal of Industrial Engineering International, vol. 13, no. 4 (2017), DOI: 10.1007/s40092-017-0196-8.

[9] Zhonghua Yun, Jun Jiang, *Research on Output Characteristics of Different PV Array Structures with Partial Shadow*, in 3rd International Conference on Energy, Environment and Materials Science (EEMS) ©EEMS (2017), DOI: 10.1088/1755-1315/94/1/012107.

[10] Chidurala Saiprakash, Alivarani Mohapatra, Byamakesh Nayak, Sriparna Roy Ghatak, *Analysis of partial shading effect on energy output of different solar PV array configurations*, in 3rd International Conference on Solar Energy Photovoltaics (ICSPE) ©ICSPE (2019), DOI: 10.1016/j.matpr.2020.08.307.

[11] Hao Yang, *Analysis of Output Characteristics of Photovoltaic Arrays Under Shaded Conditions*, in 7th International Conference on Communications, Signal Processing, and Systems (CSPS) ©CSPS (2018), DOI: 10.1007/978-981-13-6508-9_44.

[12] Mostafa Hazem H., Ibrahim Amr M., Anis Wagdi R., *A performance analysis of a hybrid golden section search methodology and a nature-inspired algorithm for MPPT in a solar PV system*, Archives of Electrical Engineering, vol. 68, no. 3, pp. 611–627 (2019), DOI: 10.24425/aee.2019.129345.

[13] Zhang Mingrui, Chen Zheyang, Wei Li, *Quantitative calculation of shadow tolerability for photovoltaic modules under different bypass diode configurations*, Acta Energiae Solaris Sinica, vol. 40, no. 07, pp. 1938–43 (2019).

[14] Lyu Shenghua, Wang Lei, Ren Chunguang, Han Xiaoqing, Guo Wenjiao, *Study on chraracteristics of series photovoltaic array and maximum power tracking under complex illumination*, Acta Energiae Solaris Sinica, vol. 38, no. 9, pp. 2329–2336.(2017).

[15] Yan Jing-bin, Tong Yao, Cao Lei, Liu Dong-Xu, Xu Yongliang, *Modeling and output characteristics simula tion of photovoltaic cells under partial shading condition*, Chinese Journal of Power Sources, vol. 42, no. 5, pp. 685–688+692 (2018).